INSTITUTE OF PHYSICS PUBLISHING PHYSICS IN MEDICINE AND BIOLOGY

Phys. Med. Biol. **50** (2005) 3927–3939 doi:10.1088/0031-9155/50/17/001

Electrophysiological measures of acute cerebral ischaemia

T C Ferree[1] **and R C Hwa**[2]

[1] Department of Radiology and Bioengineering Graduate Group, University of California, San Francisco, CA 94143, USA
[2] Institute of Theoretical Science and Department of Physics, University of Oregon, Eugene, OR 97403, USA

E-mail: tom.ferree@radiology.ucsf.edu.

Received 17 November 2004, in final form 13 June 2005
Published 11 August 2005
Online at stacks.iop.org/PMB/50/3927

Abstract

A method of EEG analysis is described which provides new insights into EEG pathology in cerebral ischaemia. The method is based on a variant of detrended fluctuation analysis (DFA), which reduces short (10 s) segments of spontaneous EEG time series to two dimensionless scaling exponents. The spatial variability of each exponent is expressed in terms of its statistical moments across EEG channels. Linear discriminant analysis combines the moments into concise indices, which distinguish normal and stroke groups remarkably well. On average over the scalp, stroke patients have larger fluctuations on the longest time scales. This is consistent with the notion of EEG slowing, but extends that notion to a wider range of time scales. The higher moments show that stroke patients have markedly reduced variability over the scalp. This contradicts the notion of a purely focal EEG scalp topography and argues instead for a highly distributed effect. In these indices, subacute patients appear further from normal than acute patients.

1. Introduction

Acute cerebral ischaemia may be treated by augmenting blood pressure and by drugs such as tissue plasminogen activator, but the therapeutic window is limited to a few hours after stroke onset. Xenon-enhanced CT (Levy *et al* 1998) and diffusion-weighted MRI (Albers 1998) are sensitive to ischaemia, but are expensive and not always available. Even when these are available, there are time windows in acute stroke care when additional information could prove useful. Scalp EEG provides information about cortical function that is complementary to radiological images and becomes abnormal immediately after a decrease in blood flow

(Tolonen *et al* 1981, Nagata 1988). Compared to radiological imaging, EEG is inexpensive and portable. Potential applications of EEG for acute stroke include early detection in ambulances and field hospitals, assessment of brain response to neurovascular treatment and continuous monitoring in intensive care units (Vespa *et al* 1999). Related applications include monitoring for ischaemia during cartotid endarterectomy and monitoring for vasospasm following subarachnoid haemorrhage (Vespa *et al* 1997).

Most previous studies of stroke-related EEG are based upon the Fourier power spectrum. Collectively, these point to increased low-frequency power and decreased high-frequency power (Nagata 1988). To account for both these features, Gotman *et al* (1973) proposed the power ratio index (PRI): the ratio of low-frequency (δ, θ) to high-frequency (α, β) power. By its definition as a ratio, the PRI is effectively normalized for differences in total power across electrodes and subjects. Zhang *et al* (2000) proposed the weighted centre of bispectrum and showed hemispheric differences in rats with induced ischaemia. Merat *et al* (2001) proposed the bispectral index, which was originally developed for anaesthesia monitoring (Sigl and Chamoun 1994). To our knowledge, no study has made group comparisons to determine whether these bispectral measures are sensitive to stroke in humans.

Recently, we developed a method of analysing short (e.g., 10 s) segments of EEG time series, which reveals scale-independent properties of EEG fluctuations and quantifies them in terms of two scaling exponents (Hwa and Ferree 2002). By their definition, scaling exponents are dimensionless and insensitive to differences in signal amplitude across electrodes and subjects. With clinical applications in mind, we also developed an efficient and intuitive approach for summarizing the spatial distributions of the scaling exponents across the scalp. The objectives of this study are to derive concise neurophysiological indices that are sensitive to cerebral ischaemia, to quantify how well these indices distinguish stroke patients from a normal control group, and to evaluate the effects of electrode reference and sampling density. An EEG measure which has robust ability to distinguish normal and stroke groups is a good starting point for monitoring.

2. Methods

2.1. Subjects

This paper reports a secondary analysis of the data published in Luu *et al* (2001). The stroke patient group consists of ten adults admitted to Sacred Heart Medical Center in Eugene, OR or Oregon Health Sciences University in Portland, OR. Data were collected by EEG scientists employed by Electrical Geodesics Inc. All procedures were approved by the internal review board of both institutions. The attending neurologist referred patients for the study if they appeared to have cortical stroke associated with mild or moderate loss of function (NIH Stroke Scale >8, or isolated hemiopsia or aphasia). Patients were excluded from the study if they were younger than 18 years of age, had open wounds of the scalp, haemorrhagic stroke, craniotomy defects, tumours or other intracranial lesions visible in CT, recent use of barbiturates, benzodiazerpines, lithium, tricyclics, neuroleptic medications or were given medications as part of stroke care that were judged to have possible effects on EEG. Patients were not excluded on the basis of sex, gender, ethnicity or socioeconomic background.

The control group consists of 18 healthy adults, without previous history of stroke, seizure or head trauma. Most control subjects were recruited from a senior center in Eugene, OR, thus the two groups are approximately age-matched. An MRI was collected for each control subject, to confirm lack of infarcts or structural abnormalities.

2.2. EEG acquisition

Data were recorded using a 128-channel EEG system (Electrical Geodesics Inc.). This system uses saline-moistened sponges in a tensioned structure to allow rapid (5–10 min) application of a large number of channels in clinical settings. The reference electrode is located at the vertex and the isolated common at the nasion. The amplifiers were set to filter in the range 0.1–100 Hz and to digitize at 250 Hz. During recording, subjects were asked to relax with eyes closed for several minutes.

For most subjects, visual inspection of the data revealed that a small number of channels were obviously in poor contact with the scalp. These were identified by eye and excluded from further analysis. The scientist who collected the data manually selected a 10 s data segment to have no visible artefacts due to eye blinks or movements and to be representative of the entire record. This selection was not biased towards our methods. In clinical applications, both bad channels and artefacts may be detected automatically (Junghofer *et al* 2000).

2.3. Detrended fluctuation analysis

Detrended fluctuation analysis (DFA) is a technique for discovering and quantifying scale-independent properties in complex systems. It was derived originally to quantify long-range correlations in nucleotides (Peng *et al* 1992). It has been applied in cardiology to study heartbeat irregularity (Peng *et al* 1993) and in EEG to study long-range correlations in alpha power (Linkenkaer-Hansen *et al* 2001). In order to characterize the temporal fluctuations in spontaneous EEG time series, without bias towards any particular spectral band, we adapted DFA to be suitable for continuous time series (Hwa and Ferree 2002). We use the term continuous here to contrast with cardiac time series, for which only the inter-beat intervals were analysed (Peng *et al* 1993).

The spirit of DFA is to define a measure of the fluctuations F on a particular time scale τ and look for power-law behaviour in $F(\tau)$. In our adaptation of DFA, the fluctuations in a discretely sampled time series are computed as follows. The time series of length N is first divided into B windows of equal size k, discarding any remainder. In this way, the fluctuations are computed on the time scale $\tau = k\Delta t$, where Δt is the sampling interval. Within each window b, let the time series be denoted by V_j and let the linear fit of V_j be denoted by $\bar{V}_j$. The squared fluctuations in this window are defined by

$$F_b^2(\tau) \equiv \frac{1}{k}\sum_{j=1}^{k}[V_j - \bar{V}_j]^2. \tag{1}$$

Averaging over the B windows leads to

$$F(\tau) = \sqrt{\frac{1}{B}\sum_{b=1}^{B} F_b^2(\tau)}. \tag{2}$$

Thus, $F(\tau)$ is a root-mean-squared measure of the fluctuations from the local linear trend in a time window of size τ. As the number of points k in each window increases, the number of windows B decreases to satisfy $Bk \leqslant N$. In our analysis, we limited $k \leqslant N/8$, to obtain a reasonable statistical average for even the longest τ and to stay within the pass band of the amplifiers.

We showed previously that short (10 s) segments of EEG time series usually exhibit power-law scaling behaviour,

$$F(\tau) \propto \tau^{\alpha}, \tag{3}$$

in two ranges of τ (Hwa and Ferree 2002). Thus, the fluctuations in each channel may be described by two scaling exponents: α_1 and α_2. The first range is $20 \leqslant \tau \leqslant 50$ ms and the second range is $130 \leqslant \tau \leqslant 1250$ ms. Of course, these ranges are not definable uniquely. Like the conventional bands of the EEG power spectrum, there is variability across channels and subjects. Nevertheless, such constructs are useful in that they provide a basis for subsequent analysis. The ranges of α_1 and α_2 were chosen by visual inspection to capture the salient and common behaviour of $\log F$ versus $\log \tau$ over all channels and subjects. Our analysis is made objective by fixing these ranges for all channels and subjects.

2.4. Moment analysis

Nearly all studies of EEG analysis for stroke have been oriented towards localization, because that can help guide clinical care. Our goal here is not localization, but rather data reduction, in order to derive concise neurophysiological indices which may be practical for rapid stroke assessment and real-time monitoring. This means reducing the data as much as possible, with a minimal loss of information in time and space. The DFA reduces the time series in each channel to two scaling exponents α_1 and α_2. In order to summarize their spatial variability, we proposed the normalized moments of their statistical distributions across the scalp (Hwa and Ferree 2002).

The first-order moments are denoted $\langle \alpha_i \rangle$, where $i = 1, 2$, and the angular brackets indicate the average over all (unrejected) channels for a single subject. As is standard in moment analysis of distributions with nonzero mean (Gardiner 1983), the higher order moments are normalized according to

$$M_q^{(i)} = \frac{\langle \alpha_i^q \rangle}{\langle \alpha_i \rangle^q}, \tag{4}$$

for $q \geqslant 2$. The normalization by $\langle \alpha_i \rangle^q$ accounts for the nonzero mean, e.g., $M_2^{(i)}$ is the square of the usual coefficient of variation plus 1.

The distributions of α_1 and α_2 across electrodes are not Gaussian and require more than two moments for their complete description. It is helpful to summarize the higher order moments in some way. We found previously that the higher order moments exhibit exponential behaviour of the form

$$M_q^{(i)} \propto \mathrm{e}^{\mu_i q}, \qquad 5 \leqslant q \leqslant 10, \tag{5}$$

where μ_i is a constant (Hwa and Ferree 2002). This behaviour is particularly sensitive to the tails of the distribution, thus a large value of μ_i indicates long tails in the distribution of α_i, e.g., as would occur if only a few channels had abnormally high or low values of α_i.

2.5. Linear discriminant analysis

The moments $\langle \alpha_i \rangle$ and $M_q^{(i)}$ are defined for α_1 and α_2 separately. In order to compare the two subject groups, we plot for each q the moments of α_2 versus α_1 in a two-dimensional scatter plot, using different symbols for the two subject groups. Visual inspection will show that the two subject groups cluster according to *both* α_1 and α_2.

For each q, we use linear discriminant analysis to fit the separation between groups. The resulting discriminant index is associated with a separatrix, a line drawn between the two groups, along which the probability of membership in either group is equal and the discriminant index is constant. In this way, the discriminant index parametrizes the difference between the groups along a line perpendicular to the separatrix. For the purpose of defining

an index, all lines parallel to the separatrix are equivalent. By convention, the discriminant index is shifted to equal zero at either (0, 0) or (1, 1), depending upon the moment order q.

Linear discriminant analysis assumes that the probability distribution for each group is multivariate normal. Although that is difficult to prove for small data sets, we adopt this assumption here for simplicity. Even if the within-group distributions are not multivariate normal, the groups are so well separated that linear analysis still gives a meaningful parametrization of their difference.

2.6. Electrode reference and sampling density

The data in this study were collected with an EEG system that allows the application of 130 electrodes in 5–10 min. The reference electrode is located at the vertex, in order to ensure good contact. We now address two practical issues related to these facts.

The physics of voltage measurement on the scalp implies that the signal in each channel is influenced by brain activity under both the measurement and reference electrode equally (Rush and Driscoll 1969). Unfortunately, no location on the head provides a truly quiet reference. In order to assess reference effects on our analysis, we applied DFA to vertex-referenced and average-referenced data. The average reference is obtained at each time point by subtracting the mean voltage across all (unrejected) scalp electrodes. With adequate spatial sampling, this sum approximates the surface integral and the resulting average-referenced data approximate the voltage relative to infinity (Nunez 1981). Of course, the scalp surface integral cannot be determined precisely, due to finite electrode sampling density and incomplete head coverage, but even with its imperfections, the average-referenced potential has the desirable feature that it is independent of any explicit choice of reference electrode.

It is well established that EEG systems with less than 64 electrodes inadequately sample the spatial variations in scalp EEG (Srinivasan *et al* 1998), yet most clinics still use the 10–20 system with only 18 channels. In order to assess the effects of spatial sampling density, we sub-sampled our 128-channel data to the 18 electrode locations of the standard 10–20 montage. We present results for four cases: case 1 is average reference, 128 channels; case 2 is average reference, 18 channels; case 3 is vertex reference, 128 channels; case 4 is vertex reference, 18 channels. To compute the average reference in case 2, we used only the 18 channels that would be available experimentally.

3. Results

3.1. Moment analysis

Figure 1 shows the results of moment analysis for case 1: 128 channels, average reference. In each plot, the two groups appear clearly distinct. There are two main observations that broaden our understanding of how stroke is reflected in scalp EEG. First, stroke patients have higher mean values (figure 1(a)) of *both* $\langle\alpha_1\rangle$ and $\langle\alpha_2\rangle$. This is consistent with the familiar notion of slowing, but extends that notion to a wider range of time scales. Second, stroke patients have markedly lower variability (figures 1(b) and (c)) across the scalp, as measured by the normalized variance. Figure 1(d) shows the exponential behaviour of the higher moments, confirming this result. This is inconsistent with a purely focal scalp topography, yet the difference between groups obtained with this measure is quite pronounced. These points are elaborated in section 4.

Figure 2 shows the results of moment analysis for case 2: 18 channels, average reference. Overall, the results are very similar to those for case 1. Comparing figures 1(a) and 2(a), the

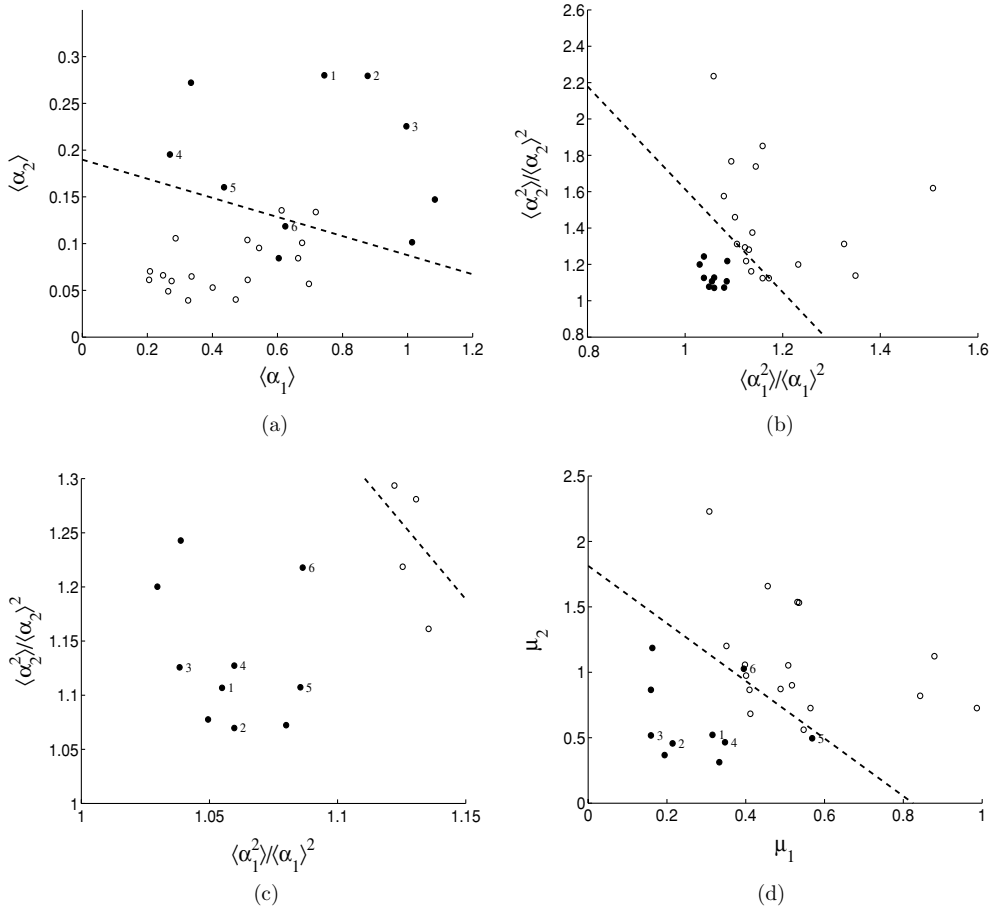

Figure 1. Results of moment analysis for case 1: average reference, 128 channels. Parts (a) and (b) show the first two moments, respectively. Part (c) is merely a zoomed version of (b). Part (d) shows the exponents describing the higher moments $5 \leqslant q \leqslant 10$. Open circles indicate control subjects; filled circles indicate stroke patients. Dashed lines indicate the separatrix defined by linear discriminant analysis. Numerical labels indicate the six patients for whom the time from stroke onset is known; these correspond exactly to the patient labels in Luu *et al* (2001).

means $\langle\alpha_1\rangle$ and $\langle\alpha_2\rangle$ are quite robust to spatial under-sampling. Comparing figures 1(b) and 2(b), the normalized variances still reveal the group differences well, with the exception that one stroke subject falls within the normal group in figure 2(b). Comparing figures 1(b)–(d) and 2(b)–(d), there appears a tendency for the estimates of variability to be smaller with only 18 channels. This is expected because under-sampling results in missing the tails of a distribution, and higher moments are more sensitive to the tails.

Figure 3 shows the results of moment analysis for case 3: 128 channels, vertex reference. The results are similar to case 1, with one notable difference. Comparing figures 1(b)–(d) and 3(b)–(d), the normal and stroke groups are better separated using the average reference; subject 6 falls within the normal group using vertex reference. It is difficult to know from these results whether this is truly a reference effect or a consequence of statistical variability within the data and analysis methods. Nevertheless, we expect the average reference to perform better and that prediction is supported by these results (see table 1).

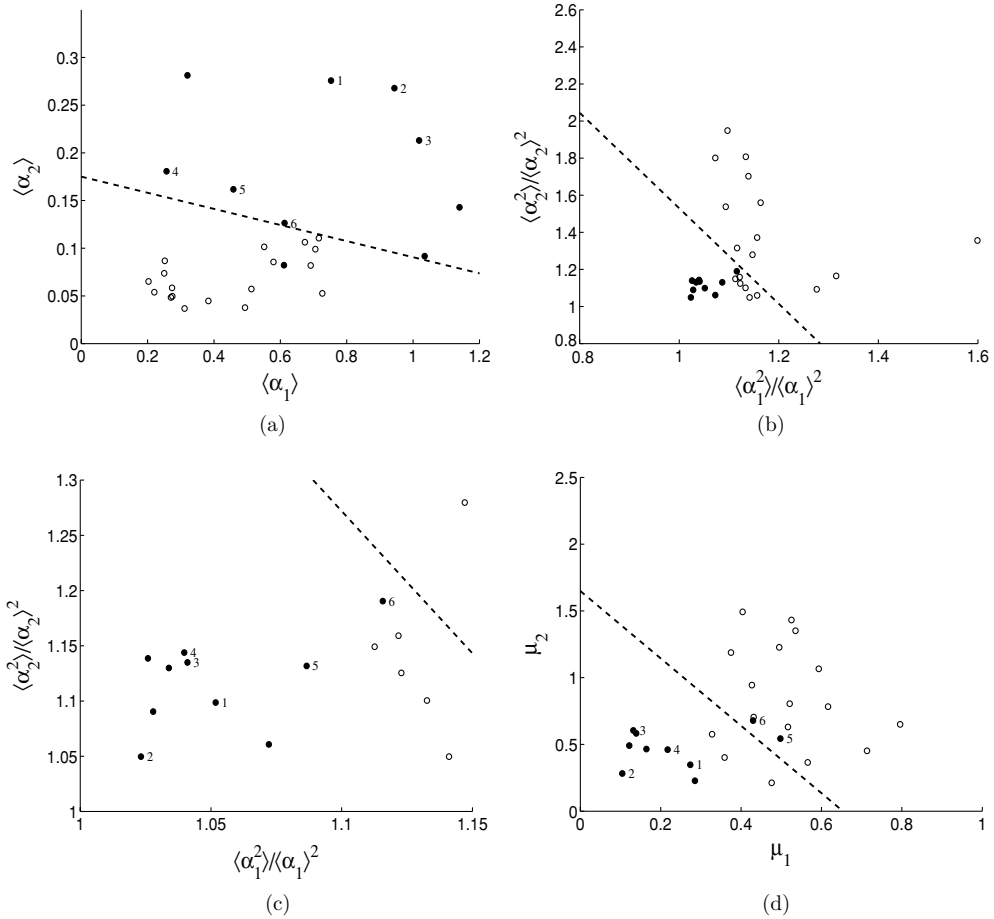

Figure 2. Results of moment analysis for case 2: average reference, 18 channels. Symbols are the same as in figure 1.

Table 1. Performance of neurophysiological indices.

Case	N_{ch}	Reference	p_R ($\times 10^{-4}$)	p_S ($\times 10^{-4}$)	p_T ($\times 10^{-4}$)
1	128	Average	2.44	0.03	0.04
2	18	Average	2.15	0.08	0.03
3	128	Vertex	5.53	1.12	0.13
4	18	Vertex	4.31	0.24	4.89

Figure 4 shows the results of moment analysis for case 4: 18 channels, vertex reference. Figure 4(a) is almost identical to figure 3(a), reinforcing that the means are robust to spatial under-sampling. Comparing figures 3(b)–(d) and 4(b)–(d), even the higher moments appear surprisingly robust to spatial under-sampling, although the group separation is somewhat better with more channels.

The numbers to the right of the filled circles in figures 1–4 show the subject numbers of the six patients in Luu *et al* (2001), for whom the time of stroke onset is known. Patients 1–3

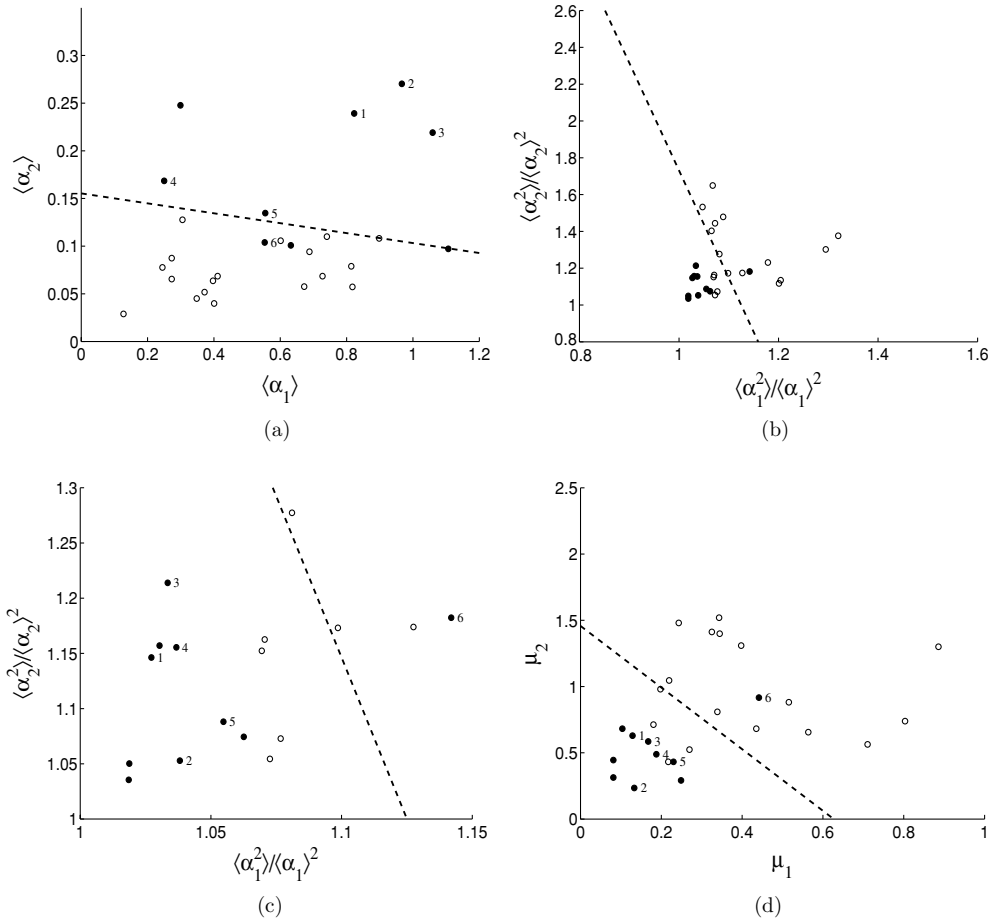

Figure 3. Results of moment analysis for case 3: vertex reference, 128 channels. Symbols are the same as in figures 1 and 2.

are subacute: the EEG data were acquired within 24–36 h of stroke onset. Patients 4–6 are acute: the EEG data were collected within 4–9 h of stroke onset. All these patients are outside the therapeutic window when the most rapid changes normally occur, yet all four figures are consistent in suggesting that acute and subacute patients cluster differently relative to the separatrix. Although the number of patients is small, we take this as a promising indication that this approach is sensitive to stroke progression from the acute to subacute stages and may be sensitive to stroke progression much earlier. Certainly, this is consistent with clinical observations that cognitive function evolves over minutes, hours and days following stroke.

3.2. Stroke indices

Linear discriminant analysis yields a separatrix, along which the value of the discriminant index is constant. The separatrices are shown as dashed lines in figures 1–4. We now provide explicit formulae for the discriminant indices, derived from the first, second and

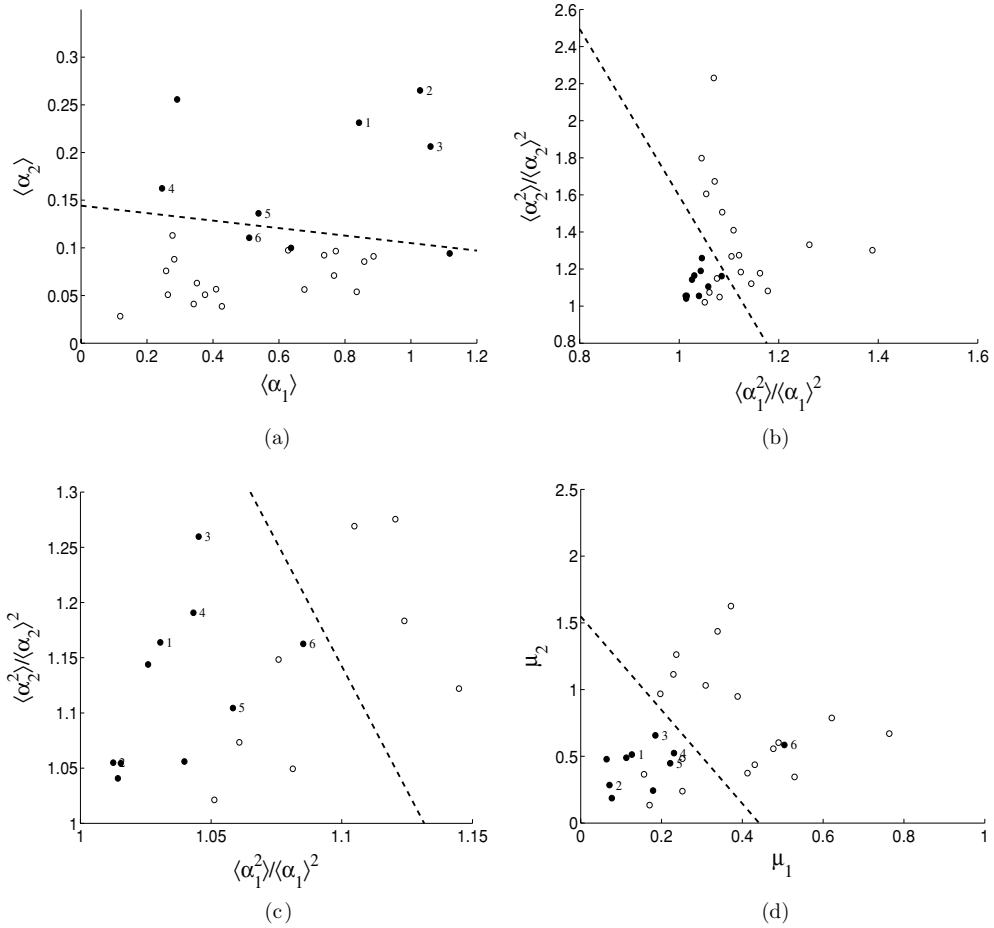

Figure 4. Results of moment analysis for case 4: vertex reference, 18 channels. Symbols are the same as in figures 1–3.

higher moments. Based on its performance, we limit our attention to case 1; the formulae for case 2 are quite similar. The means (figure 1(a)) yield the index

$$R = 4.3\langle\alpha_1\rangle + 42\langle\alpha_2\rangle. \tag{6}$$

The normalized variances (figure 1(b)) yield the index

$$S = 17\langle\alpha_1^2\rangle/\langle\alpha_1\rangle^2 + 6\langle\alpha_2^2\rangle/\langle\alpha_2\rangle^2 - 23. \tag{7}$$

The exponential behaviours of the higher moments (figure 1(d)) yield the index

$$T = 7.6\mu_1 + 3.5\mu_2. \tag{8}$$

For the purpose of parametrizing the difference between the two groups, all lines parallel to the separatrix are equivalent. For easy graphical interpretation, we define these indices to vanish at the point (0, 0) for the first and higher moments, and (1, 1) for the second moments.

This approach allows the spatial statistics of the temporal fluctuations of scalp EEG to be described concisely in terms of the indices R, S and T. Figure 5 shows the number of subjects in each group, with values of R and S falling in various bins. Overall, stroke patients have

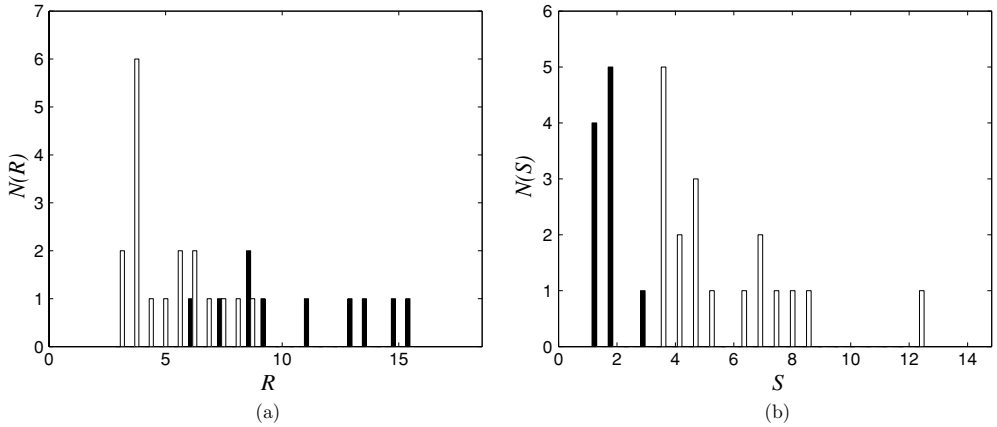

Figure 5. Histograms of the discriminant indices R and S, computed for case 1. Open bars represent normal subjects; filled bars represent stroke patients.

larger R and smaller S. As expected from figure 1, the two groups overlap in the index R, but are well separated in the index S. It may be possible to combine R and S into a single composite index or to apply multivariate analysis to the moments directly, but these ideas are not pursued here. The advantage of the present approach is that different moment orders can be interpreted simply as the spatial mean and variability, and these have interpretable differences across subject groups and spatial sampling densities.

In order to quantify the effectiveness of each index for distinguishing normal and stroke groups, we performed a t-test with the null hypothesis that the two groups are one. Table 1 shows the probability that the null hypothesis is true.

We find $p < 0.001$ throughout, thus it would be reasonable to say that all indices are quite successful at this discrimination task. Yet, success at the group level does not imply adequate sensitivity to track changes in a single subject. To that end, we make the following qualitative assessments. The mean index R performs well in all cases and best in cases 1 and 2 based upon the average reference. The variability indices S and T generally perform much better and best in cases 1 and 2. The results are more sensitive to reference electrode than to sampling density. Overall, the average reference performs better than vertex reference.

4. Discussion

4.1. Summary

We have described a principled approach to the dynamical analysis of spontaneous EEG data. It requires only short data (10 s) segments, yet integrates information across a wide range of temporal and spatial scales accessible with scalp EEG. In the time domain, detrended fluctuations analysis (DFA) represents the scaling behaviour in each channel as two dimensionless exponents α_1 and α_2. In the spatial domain, the moments of the distributions of α_1 and α_2 summarize the mean and variability across the scalp. For each order q, the two moments corresponding to the time ranges fit by α_1 and α_2 summarize the entire EEG data set as a single point in two dimensions. Linear discriminant analysis reduces the data further to three indices: R, S and T, each separating the groups along a line. The indices appear robust to spatial under-sampling, which makes them compatible with most clinical EEG systems.

Based on their sensitivity to the difference between groups, we suggest these indices may prove useful clinically.

4.2. Temporal slowing

When DFA was first applied in physiology, it was applied to the discrete time series of intervals between heartbeats (Peng *et al* 1993). The time series was first mean-subtracted, then integrated, before applying equations (1) and (2). Integration has the effect of smoothing the interval time series to be more like a continuous one and subtracting the mean avoids a spurious linear growth of the integral. Because EEG time series are already continuous and integration acts as a low-pass filter, that seems unjustified in this context, so we adapted DFA by applying equations (1) and (2) directly without integration (Hwa and Ferree 2002). Subtracting the mean is not necessary, because the local linear fit $\bar{V}_j$ in (1) removes it automatically. This approach reveals a vivid scaling behaviour in short segments of spontaneous EEG time series.

In the original formulation of DFA, there exists an analytic relationship between $F(\tau)$ and the Fourier power spectrum $P(f)$ (Heneghan and McDarby 2000, Rangarajan and Ding 2000). In our adaptation of DFA, a similar relationship also exists (Ferree and Hwa 2003, Robinson 2003). According to (3), linearity reflects scaling behaviour within a given range. The exponents α_1 and α_2 are defined to match the piecewise linear behaviour in plots of log F versus log τ. The violation of linearity between these two ranges implies an intrinsic time scale in the data. Not surprisingly, the time scale $\tau \simeq 0.1$ s between the two linear ranges is that of the prominent human α-rhythm near $f \simeq 10$ Hz. The time range defining α_1 encompasses the β and γ bands, and that defining α_2 encompasses the δ and θ bands.

The numerical value of α_i reflects the relative size of fluctuations across its range; a large value of α_i implies relatively larger fluctuations on the longest time scales within that range. Returning to the correspondence with the Fourier power spectrum, loosely speaking, large α_1 suggests a large ratio of β to γ power, while large α_2 suggests a large ratio of δ to θ power. From this viewpoint, the finding of larger $\langle\alpha_2\rangle$ is consistent with the conventional notion of EEG slowing. The finding of larger $\langle\alpha_1\rangle$ was not predicted, but nevertheless contributes significantly to the index R, and thus extends the notion of slowing to include the β and γ bands. We speculate that clinical observations of slowing have been associated mainly with the δ and θ bands, because those bands are most easily visualized in chart recordings. Yet, many studies have pointed to the effects of stroke on higher frequency bands (e.g., Gotman *et al* 1973) and our findings are consistent with these.

4.3. Local versus global effects

In most applications of EEG to stroke, it has been viewed that stroke-related EEG changes should occur locally and reveal the location of the lesion (Nagata 1988, Luu *et al* 2001). This view is supported by radiological images in which lesions are seen as spatially compact. It is also intuitive because the ischaemic penumbra is known to generate pathological EEG in the very acute phase. On the other hand, the affected area of cortex is connected directly to remote brain areas via cortico-cortical fibres and connected indirectly to virtually all other brain areas via small-world topologies (Sporns and Zwi 2004), thus it is not certain that the effects of stroke on scalp EEG should be limited to just a few electrodes above the lesion. Indeed, there are many reports to the contrary, usually labelled diaschisis. Bilateral decrease in blood flow (Hoedt-Rasmussen and Skinhoj 1964, Rubin *et al* 2000), contralateral changes in electrical activity (Kempinsky 1958, Juhasz *et al* 1997) and sleep EEG (Muller *et al* 2002), changes in transhemispheric excitability (Reinecke *et al* 1999, Butefisch *et al* 2003) and studies of stroke

recovery (Seitz *et al* 1999), all suggest that the effect of stroke on the EEG is not limited to electrodes located over the lesion, but includes distant locations as well.

Our findings suggest that the effects of stroke on scaling measures of scalp EEG are highly distributed, not purely local. If stroke pathophysiology were reflected as an increase or decrease in the scaling exponents of a few channels only, those channels would appear as outliers in the distributions over the scalp. We demonstrated previously that a small number of channels cannot possibly account for the observed increase in the means, given the observed ranges of the scaling exponents themselves (Hwa *et al* 2003). We showed here that the variability is drastically decreased, which implies further that the increase must be distributed over many electrodes. We refer to this as a *global* effect of stroke on scalp EEG. We appreciate that stroke localization remains a desirable goal and that such knowledge could help guide treatment. Indeed, focal effects of stroke on scalp EEG have been reported in these very same data (Luu *et al* 2001), but the finding of focal slowing has proven inadequate to distinguish normal and stroke groups (Nagata 1988), in part because focal patterns of low-frequency activity can occur in healthy brains. We suggest that the methods presented here, which readily distinguish normal and stroke groups, hold promise of adequate sensitivity to contribute to early detection and continuous monitoring.

4.4. Stroke progression

The data provided for this study were collected either 4–9 h (acute) or 24–36 h (subacute) after stroke onset. We suggested that R, S and T may reflect stroke progression, because the acute and subacute patients appear to cluster differently relative to the control group. It may seem odd that the more acute patients fall closer to the control group, but this may simply reflect the nature of gradual changes that continue to occur from hours to days. It may be that the effects of stroke are local in the first hours and become more global on longer time scales, so that the patient traces out a trajectory in the space of these indices. Understanding that trajectory could potentially inform clinicians about stroke severity and rate of progression. In order to demonstrate that, it is desirable to collect EEG data multiple times in the emergency room and ICU, and to correlate these indices with radiological images and neuropsychological exams.

Acknowledgments

The authors thank Phan Luu and Don Tucker for providing data for our analysis, Wei He and Ying Lu for computational assistance, and Wade Smith, Michael Aminoff and Curtis Benesch for helpful discussions. This work was supported in part by the National Institutes of Health under grant nos R44-NS-38829 and R01-NS-27900, and the US Department of Energy under grant no DE-FG03-96ER40972.

References

Albers G W 1998 Diffusion-weighted MRI for evaluation of acute stroke *Neurology* **51** S47–9

Butefisch C M, Netz J, Wessling M, Seitz R J and Homberg V 2003 Remote changes in cortical excitability after stroke *Brain* **126** 470–81

Ferree T C and Hwa R C 2003 Power-law scaling in human EEG: relation to Fourier power spectrum *Neurocomputing* **52–54** 755–61

Gardiner C W 1983 *Handbook of Stochastic Methods* (Berlin: Springer)

Gotman J, Skuce D R, Thompson C J, Gloor P, Ives J R and Ray W F 1973 Clinical application of spectral analysis extraction of features from electroencephalograms with slow waves in adult patients *Electroencephalogr. Clin. Neurophysiol.* **35** 225–35

Heneghan C and McDarby G 2000 Establishing the relationship between detrended fluctuation analysis and power spectral density analysis for stochastic processes *Phys. Rev.* E **62** 6103–10

Hoedt-Rasmussen K and Skinhoj E 1964 Transneural depression of the cerebral hemispheric metabolism in man *Acta Neurol. Scand.* **40** 41–6

Hwa R C and Ferree T C 2002 Scaling properties of fluctuations in the human electroencephalogram *Phys. Rev.* E **66** 021901

Hwa R C, He W and Ferree T C 2003 The global effects of stroke on human electroencephalogram *J. Integr. Neurosci.* **2** 45–53

Juhasz C, Kamondi A and Szirmai I 1997 Spectral EEG analysis following hemispheric stroke: evidences of transhemispheric diaschisis *Acta Neurol. Scand.* **96** 397–400

Junghofer M, Elbert T, Tucker D M and Rockstroh B 2000 Statistical control of artifacts in dense-array EEG/MEG studies *Psychophysiology* **37** 523–32

Kempinsky W H 1958 Experimental study of distant effects of acute focal brain injury *Arch. Neurol. Psychiatry* **79** 376–89

Levy E I, Scarrow A M, Kanal E, Rubin G, Yonas H and Kirby L 1998 Reversible ischemia determined by xenon-enhanced CT after 90 min of complete basilar artery occlusion *Am. J. Neuroradiol.* **19** 1943–6

Linkenkaer-Hansen K, Nikouline V V, Palva J M and Ilmoniemi R J 2001 Long-range temporal correlations and scaling behavior in human brain oscillations *J. Neurosci.* **21** 1370–7

Luu P, Tucker D M, Englander R, Lockfeld A, Lutsep H and Oken B 2001 Localizing acute stroke related EEG changes: assessing the effects of spatial undersampling *J. Clin. Neurophys.* **18** 302–17

Merat S, Levecque J P, Le Gulluche Y, Diraison Y, Brinquin L and Hoffmann J J 2001 BIS monitoring may allow the detection of severe cerebral ischemia *Can. J. Anaesth.* **48** 1066–9

Muller C, Achermann P, Bischof M, Nirkko A C, Roth C and Bassetti C L 2002 Visual and spectral analysis of sleep EEG in acute hemispheric stroke *Eur. Neurol.* **48** 164–71

Nagata K 1988 Topographic EEG in brain ischemia: correlation with blood flow and metabolism *Brain Topogr.* **1** 97–106

Nunez P L 1981 *Electric Fields of the Brain* (Oxford: Oxford University Press)

Peng C K, Buldyrev S, Goldberger A L, Havlin S, Sciortino F, Simons M and Stanley H E 1992 Long-range correlations in nucleotide sequences *Nature* **356** 168–70

Peng C K, Mietus J, Hausdorff J M, Havlin S, Stanley H E and Goldberger L 1993 Long-range anticorrelation and non-Gaussian behavior of the heartbeat *Phys. Rev. Lett.* **70** 1343–6

Rangarajan G and Ding M 2000 Integrated approach to the assessment of long-range correlation in time series data *Phys. Rev.* E **61** 4991–5001

Reinecke S, Lutzenburg M, Hagemann G, Bruehl C, Neumann-Haefelin T and Witte O W 1999 Electrophysiological transcortical diaschisis after middle cerebral artery occlusion (MCAO) in rats *Neurosci. Lett.* **261** 85–8

Robinson P A 2003 Interpretation of scaling properties of electroencephalographic fluctuations via spectral analysis and underlying physiology *Phys. Rev.* E **67** 032902

Rubin G, Levy E I, Scarrow A M, Firlik A D, Karakus A, Wechsler L, Jungreis C A and Yonas H 2000 Remote effects of acute ischemic stroke: a xenon CT cerebral blood flow study *Cerebrovasc. Dis.* **10** 221–8

Rush S and Driscoll D A 1969 EEG electrode sensitivity—an application of reciprocity *IEEE Trans. Biomed. Eng.* **16** 15–22

Seitz R J, Azari N P, Knorr U, Binkofski F, Herzog H and Freund H J 1999 The role of diaschisis in stroke recovery *Stroke* **30** 1844–50

Sigl J C and Chamoun N G 1994 An introduction to bispectral analysis for the EEG *J. Clin. Monit.* **10** 392–404

Sporns O and Zwi J D 2004 The small world of the cerebral cortex *Neuroinformatics* **2** 145–62

Srinivasan R, Tucker D M and Murias M 1998 Estimating the spatial Nyquist of the human EEG *Behav. Res. Methods Instrum. Comput.* **30** 8–19

Tolonen U, Ahonen A, Sulg I A, Kuikka J, Kallanranta T, Koskinen M and Hokkanen E 1981 Serial measurements of quantitative EEG and cerebral blood flow and circulation time after brain infarction *Acta Neurol. Scand.* **63** 145–55

Vespa P M, Nenov V and Nuwer M R 1999 Continuous EEG monitoring in the intensive care unit: early findings and clinical efficacy *J. Clin. Neurophysiol.* **16** 1–13

Vespa P M, Nuwer M R, Juhasz C, Alexander M, Nenov V, Martin N and Becker D P 1997 Early detection of vasospasm after acute subarachnoid hemorrhage using continuous EEG ICU monitoring *Electroencephalogr. Clin. Neurophysiol.* **103** 607–15

Zhang J-W, Zheng C-X and Xie A 2000 Bispectrum analysis of focal ischemic cerebral EEG signal using third-order recursion method *IEEE Trans. Biomed. Eng.* **47** 352–9